

AVO inversion through iteration of direct nonlinear inverse formulas

Tiansheng Chen and Kris Innanen

ABSTRACT

Linear AVO inversion technique has been used widely in industry to invert elastic parameter. In this paper, I put forward a new inversion through iteration of direct nonlinear inverse formulas. Following the workflow presented by Innanen (Innanen 2011), I expand the reflection coefficient of PP wave and PS wave as function of elastic parameters contrast at third order. Those formulae can be used to invert elastic parameter by use of AVO series reversion method or Gauss-Newton iteration method. To solve the local convergence problem of Gauss-Newton iteration method, we introduce the first or second AVO series reversion result as the initial value. All of the experiments illustrate that reconstruction of contrasts from Gauss-Newton iteration of direct nonlinear inverse formulas is more accuracy and faster.

INTRODUCTION

AVO (Amplitude vary with offset) analysis and inversion have been used widely to characterize the elastic parameters and rock and fluid properties subsurface. The Zoeppritz equation (Zoeppritz 1919) is the fundamental mathematical formula for the amplitudes of reflected and transmitted plane waves when an incident P-wave strikes an welded elastic boundary. Although it gives precise values of the amplitudes of the reflected and transmitted plane waves, the difficulty in understanding the effects of parameter changes on the seismic amplitudes and the unstable solution resulting from its intrinsic nonlinearity prevent it from application. In contrast, The linearized approximation to the Zoeppritz equations is the basis of AVO analysis and prestack inversion (Ikelle, 1995; Buland and Omre, 2003; Yin et al., 2008). Smith and Gidlow (Smith and Gidlow 1987) are the first to develop a P- and S-wave velocity reflectivity inversion method based on P-wave AVO variation. Goodway et al. (Goodway 1999) propose lambda-mu-rho (LMR) technology for fluid discrimination, but it has some limits for practical reservoirs in porous media. Stewart (1996) described a similar method to derive estimates of shear velocity and density directly from PS wave. Stewart (1990) outlined a procedure that incorporates both P-P and P-S seismic gathers in a joint P-P and P-S inversion. Smith (Smith,1996) extended the weighted-stacking method to the case of three-parameter inversion. The three elastic parameters would be either P-wave velocity contrast, S-wave velocity contrast and density contrast or P-wave impedance contrast, S-wave impedance contrast. Lines (Lines 1998) further showed that density determination is difficult for limited apertures (limited incidence angles) and typical seismic velocities. Downton (Downton 2005) constrain three-parameter AVO inversion with probabilistic constraints on local geology, and he also estimates reliable density reflectivity. Jin et al. (Jin, Cambois, and Vuillermoz 2000) use singular value decomposition to stabilize the linearized P-SV reflection equations and to obtain reasonable results for synthetic and field data. Russell et al. (Russell et al. 2003) derive the fluid component which is the real factor that reflects the influence of fluid in porous rock. EI inversion (Connolly 1999) provided a consistent framework to calibrate and invert nonzero-offset seismic data just as the acoustic impedance inversion. However, according to Snell's law, the incident and transmitted angle at each side of interface are different. The ray impedance concept (Wang 2003) remained constant at both sides of interface. Zhang (Zhang and Wang 2010) applied ray impedance inversion to tight-sand gas reservoir prediction and showed that ray impedance was superior than acoustic impedance, elastic impedance and shear impedance in identifying fracture zone and the characterization of reservoir distribution. Larsen (Larsen 1999) introduced global searching using the iterative nonlinear algorithm to invert the exact Zoeppritz equations solution for PP and PS reflectivity and improved the accuracy for

elastic parameter estimates. Chen and Wei (Chen and Wei, 2012) produced Zoeppritz-based joint AVO inversion of PP and PS waves in Ray parameter domain.

All the linear method is based on the first linear approximation to exact Zoeppritz equation under the condition that the incident is small and the contrasts in elastic parameters is much less than unity. Iterative nonlinear inversion based on exact Zoeppritz equation is model matching problem in sense which update the properties model to minimize the difference between forward synthetic data and measured data. Based on inverse scattering theory, Zhang and Weglein (Zhang and Weglein 2009) proposed direct nonlinear inversion. The equation for the linear estimate is the exact equation for the linear estimate. The equation for the quadratic estimate is the exact equation for the quadratic estimate, and so on for each higher term. There is no iteration, no cost function, no model matching, but an order by order in the data direct solution, where each step is exact for its indicated order of approximation. Innanen (Innanen 2011) extend the inverse scattering series work to frequency dependent prestack AVO inversion holding for both two parameter anacoustic problems and five parameter anelastic problems.

In this paper, following the workflow presented by Innanen (Innanen 2011), I develop a new method of direct nonlinear inversion of contrasts in elastic parameter rather than parameter perturbations and compare the direct nonlinear inversion (i.e. series reversion) and iterative nonlinear inversion.

BASIC THEORY AND FORMULAS

For an isotropic elastic medium, when we consider a plane P wave obliquely incident upon a welded interface boundary, the Zoeppritz equation describes the amplitude relation between incident wave and scatter wave under the condition of continuous stress and displacement. For convenient, following the theory of Knott-Zoeppritz equations, we have

$$M \begin{bmatrix} R_{pp} \\ R_{ps} \\ T_{pp} \\ T_{ps} \end{bmatrix} = N \quad (1)$$

Where

$$M = \begin{bmatrix} -X & -(1-B^2X^2)^{\frac{1}{2}} & CX & -(1-D^2X^2)^{\frac{1}{2}} \\ (1-X^2)^{\frac{1}{2}} & -BX & (1-C^2X^2)^{\frac{1}{2}} & DX \\ 2B^2X(1-X^2)^{\frac{1}{2}} & B(1-B^2X^2) & 2AD^2X(1-C^2X^2)^{\frac{1}{2}} & -AD(1-2D^2X^2) \\ -(1-2B^2X^2) & 2B^2X(1-B^2X^2)^{\frac{1}{2}} & AC(1-2D^2X^2) & 2AD^2(1-D^2X^2)^{\frac{1}{2}} \end{bmatrix} \quad (2)$$

$$N = \begin{bmatrix} X \\ (1-X^2)^{\frac{1}{2}} \\ 2B^2X(1-X^2)^{\frac{1}{2}} \\ 1-2B^2X^2 \end{bmatrix} \quad (3)$$

and where $X = \sin \theta$ is sinusoidal function of incident angle θ and constant parameters A through D denote the elastic parameters ratios

$$A = \frac{\rho_2}{\rho_1}, B = \frac{\beta_1}{\alpha_1}, C = \frac{\alpha_2}{\alpha_1}, D = \frac{\beta_2}{\alpha_1} = B \frac{\beta_2}{\beta_1} \quad (4)$$

Any one of the four displacement reflection coefficients can be solved from the equations using Cramer's rule. Forming two auxiliary matrixes M_p and M_s by replacing the first and second columns of M with N , the solutions are obtained

$$R_{pp} = \frac{\det(M_p)}{\det(M)}, R_{ps} = \frac{\det(M_s)}{\det(M)} \quad (5)$$

In order to understand the response of the reflection coefficient R_{pp} and R_{ps} to contrasts in elastic parameters across the interface, we rewrite elastic parameter ratios in terms of elastic parameter contrasts.

$$A = \frac{\rho_2}{\rho_1} = 1 + r_\rho + \frac{1}{2}r_\rho^2 + \frac{1}{4}r_\rho^3 + \dots \quad (6)$$

$$C = \frac{\alpha_2}{\alpha_1} = 1 + r_\alpha + \frac{1}{2}r_\alpha^2 + \frac{1}{4}r_\alpha^3 + \dots \quad (7)$$

$$D = \frac{\beta_2}{\alpha_1} = B \frac{\beta_2}{\beta_1} = B \left[1 + r_\beta + \frac{1}{2}r_\beta^2 + \frac{1}{4}r_\beta^3 + \dots \right] \quad (8)$$

where $r_\alpha = \Delta\alpha/\alpha$ is the ratio of difference of P wave velocity to average of P wave velocity, $r_\beta = \Delta\beta/\beta$ is the ratio of difference of S wave velocity to average of S wave velocity and $r_\rho = \Delta\rho/\rho$ is the ratio of difference of density to average of density.

Because the parameter B is only the ratio of the incident medium parameter, we do not expand it. The square root terms involving parameter ratio A through D is also expanded by making use of the expression

$$(1-x)^{\frac{1}{2}} = 1 - \frac{1}{2}x^2 - \frac{1}{8}x^4 + \dots \quad (9)$$

When the All of the expand series are further substituted into the coefficient matrix M and auxiliary matrixes M_p and M_s , all the elements are directly expressed as series in powers of the elastic contrasts. The determinate of the matrix is a linear combination of the elements of the matrix. Therefore, if the elements of the matrix are series in orders of the elastic contrasts, so determinants can be recast in terms of elastic contrast as following

$$\det M = (\det M)_0 + (\det M)_1 + (\det M)_2 + (\det M)_3 + \dots \quad (10)$$

$$\det M_p = (\det M_p)_0 + (\det M_p)_1 + (\det M_p)_2 + (\det M_p)_3 + \dots \quad (11)$$

$$\det M_s = (\det M_s)_0 + (\det M_s)_1 + (\det M_s)_2 + (\det M_s)_3 + \dots \quad (12)$$

Where the subscript refers to order in combination of the elastic contrasts. In carrying out the expansion, one notices that the zero order of auxiliary matrix $(\det M_p)_0$ and $(\det M_s)_0$ disappear. Dividing the numerator and denominator by the zero order term in $\det M$, the reflection coefficient are rewritten as

$$R_{pp} = \frac{\det M_p}{\det M} = \frac{(\det M_p)_1 + (\det M_p)_2 + (\det M_p)_3 + \dots}{(\det M)_0 + (\det M)_1 + (\det M)_2 + (\det M)_3 + \dots}$$

$$\begin{aligned} & \frac{(\det Mp)_1}{(\det M)_0} + \frac{(\det Mp)_2}{(\det M)_0} + \frac{(\det Mp)_3}{(\det M)_0} + \dots \\ &= \frac{(\det M)_1 + (\det M)_2 + (\det M)_3 + \dots}{1 + \frac{(\det M)_1 + (\det M)_2 + (\det M)_3 + \dots}{(\det M)_0}} \end{aligned} \quad (13)$$

$$\begin{aligned} R_{ps} &= \frac{\det Ms}{\det M} = \frac{(\det Ms)_1 + (\det Ms)_2 + (\det Ms)_3 + \dots}{(\det M)_0 + (\det M)_1 + (\det M)_2 + (\det M)_3 + \dots} \\ &= \frac{\frac{(\det Ms)_1}{(\det M)_0} + \frac{(\det Ms)_2}{(\det M)_0} + \frac{(\det Ms)_3}{(\det M)_0} + \dots}{1 + \frac{(\det M)_1 + (\det M)_2 + (\det M)_3 + \dots}{(\det M)_0}} \end{aligned} \quad (14)$$

By inspection of equation (13) and (14) it is clear that the denominator somewhat looks like $1+x$, where every term in x is at least first order in terms of elastic contrasts. For small contrasts and small angle, we may reasonably assume them to be less than unity and expand the reflection coefficient as

$$R_{pp} = R_{pp1} + R_{pp2} + R_{pp3} + \dots \quad (15)$$

$$R_{ps} = R_{ps1} + R_{ps2} + R_{ps3} + \dots \quad (16)$$

Where the first order contribution to R_{pp} is

$$R_{pp1} = \frac{(\det Mp)_1}{(\det M)_0} \quad (17)$$

the second order contribution to R_{pp} is

$$R_{pp2} = \frac{(\det Mp)_2}{(\det M)_0} - \frac{(\det Mp)_1}{(\det M)_0} \frac{(\det M)_1}{(\det M)_0} \quad (18)$$

the third order contribution to R_{pp} is

$$R_{pp3} = -\frac{(\det Mp)_1}{(\det M)_0} \frac{(\det M)_2}{(\det M)_0} - \frac{(\det Mp)_2}{(\det M)_0} \frac{(\det M)_1}{(\det M)_0} + \frac{(\det Mp)_1}{(\det M)_0} \left(\frac{(\det M)_1}{(\det M)_0} \right)^2 \quad (19)$$

the first order contribution to R_{ps} is

$$R_{ps1} = \frac{(\det Ms)_1}{(\det M)_0} \quad (20)$$

the second order contribution to R_{ps} is

$$R_{ps2} = \frac{(\det Ms)_2}{(\det M)_0} - \frac{(\det Ms)_1}{(\det M)_0} \frac{(\det M)_1}{(\det M)_0} \quad (21)$$

the third order contribution to R_{ps} is

$$R_{ps3} = -\frac{(\det Ms)_1}{(\det M)_0} \frac{(\det M)_2}{(\det M)_0} - \frac{(\det Ms)_2}{(\det M)_0} \frac{(\det M)_1}{(\det M)_0} + \frac{(\det Ms)_1}{(\det M)_0} \left(\frac{(\det M)_1}{(\det M)_0} \right)^2 \quad (22)$$

Substituting the equations from (6) to (9) into the equations from (15) to (21), we derive an approximation for R_{pp} and R_{ps} which is expressed in order of elastic contrasts r_α , r_β and r_ρ (the details of coefficient refer to Appendix A).

For PP wave

$$R_{pp1} = \Gamma_{\alpha 1}^p r_\alpha + \Gamma_{\beta 1}^p r_\beta + \Gamma_{\rho 1}^p r_\rho \quad (23)$$

$$R_{pp2} = \Gamma_{\alpha 2}^p r_\alpha^2 + \Gamma_{\beta 2}^p r_\beta^2 + \Gamma_{\rho 2}^p r_\rho^2 + \Gamma_{\alpha 1 \beta 1}^p r_\alpha r_\beta + \Gamma_{\alpha 1 \rho 1}^p r_\alpha r_\rho + \Gamma_{\beta 1 \rho 1}^p r_\beta r_\rho \quad (24)$$

$$R_{pp3} = \Gamma_{\alpha 3}^p r_\alpha^3 + \Gamma_{\beta 3}^p r_\beta^3 + \Gamma_{\rho 3}^p r_\rho^3 + \Gamma_{\alpha 2 \beta 1}^p r_\alpha^2 r_\beta + \Gamma_{\alpha 2 \rho 1}^p r_\alpha^2 r_\rho + \Gamma_{\beta 2 \alpha 1}^p r_\beta^2 r_\alpha + \Gamma_{\beta 2 \rho 1}^p r_\beta^2 r_\rho + \Gamma_{\rho 2 \alpha 1}^p r_\rho^2 r_\alpha + \Gamma_{\rho 2 \beta 1}^p r_\rho^2 r_\beta + \Gamma_{\alpha 1 \beta 1 \rho 1}^p r_\alpha r_\beta r_\rho \quad (25)$$

For PS wave

$$R_{ps1} = \Gamma_{\alpha 1}^s r_\alpha + \Gamma_{\beta 1}^s r_\beta + \Gamma_{\rho 1}^s r_\rho \quad (26)$$

$$R_{ps2} = \Gamma_{\alpha 2}^s r_\alpha^2 + \Gamma_{\beta 2}^s r_\beta^2 + \Gamma_{\rho 2}^s r_\rho^2 + \Gamma_{\alpha 1 \beta 1}^s r_\alpha r_\beta + \Gamma_{\alpha 1 \rho 1}^s r_\alpha r_\rho + \Gamma_{\beta 1 \rho 1}^s r_\beta r_\rho \quad (27)$$

$$R_{ps3} = \Gamma_{\alpha 3}^s r_\alpha^3 + \Gamma_{\beta 3}^s r_\beta^3 + \Gamma_{\rho 3}^s r_\rho^3 + \Gamma_{\alpha 2 \beta 1}^s r_\alpha^2 r_\beta + \Gamma_{\alpha 2 \rho 1}^s r_\alpha^2 r_\rho + \Gamma_{\beta 2 \alpha 1}^s r_\beta^2 r_\alpha + \Gamma_{\beta 2 \rho 1}^s r_\beta^2 r_\rho + \Gamma_{\rho 2 \alpha 1}^s r_\rho^2 r_\alpha + \Gamma_{\rho 2 \beta 1}^s r_\rho^2 r_\beta + \Gamma_{\alpha 1 \beta 1 \rho 1}^s r_\alpha r_\beta r_\rho \quad (28)$$

For first order of elastic contrasts, those approximation of R_{pp} and R_{ps} is similar to Aki and Richard approximations, although it is different in its detail replacing the average incident/transmission angles with only incident angle.

To take a glance at the influence of high order term of R_{pp} and R_{ps} and the accuracy of the series AVO approximation, the comparison of each truncated term with the exact solution obtained from Zoeppritz equation is demonstrated. The model with parameters P wave velocity, S wave velocity and density [α, β, ρ] are [2700m/s, 1300m/s, 2.1g/cm³] for upper media and [3000m/s, 1900m/s, 2.4g/cm³] for lower media respectively. Figure 1 shows the comparison of exact R_{pp} curve (black solid line) with the different approximation equations. The green solid line is the linear Aki&Richard approximation equation. The three red line are the series order equations derived in this paper (first order: red solid line, second order: red dot dash line, third order: red dash line). The incident angle for Aki&Richard linear equation is the average of incident and transmission, otherwise, the one for series order equations is the real incident angle. It is clear that the series order equations are more accurate than the Aki&Richard linear equation. For this model the velocity contrast is much larger ($\Delta\alpha/\alpha = 0.2581$) leads to great difference between exact R_{pp} curve and Aki&Richard linear equation which is only more accurate under assumption that small velocity contrast. Besides the replacement of average incident with incident angle is another reason. The reflection coefficient computed from Aki&Richard is consistent with that computed from first and second order truncation at normal incident angle which still deviates from the exact value. For series order equation, the second order truncation is almost same as first order truncation at small incident angle, but moves toward exact reflection coefficient. The third order truncation appears to capture the exact R_{pp} curve. The comparison of exact R_{ps} curve with the different approximation equations in figure 2 shows the same features as R_{pp} in figure 1.

Evidently, it is well known that R_{ps} is unaffected by variations in P wave velocity in first order because that the coefficient $\Gamma_{\alpha 1}$ is zero. But to high order, only the coefficients $\Gamma_{\alpha 2}$, $\Gamma_{\alpha 3}$ and $\Gamma_{\rho 2 \alpha 1}$ equal zero by inspection of equation 26, 27 and

Appendix A. Consequently, the second and third order of R_{ps} are affected by variations in P wave velocity across interface. We establish a set of the three elastic models with varying P wave velocity $\alpha_2=3000\text{m/s}$, 3500m/s and 3800m/s at lower media, but with all the other unchanged properties as model in figure 1 including velocity S wave velocity and density in upper and lower media. It's clear that changes in the P wave velocity contrast certainly affect the reflection coefficient of PS wave.

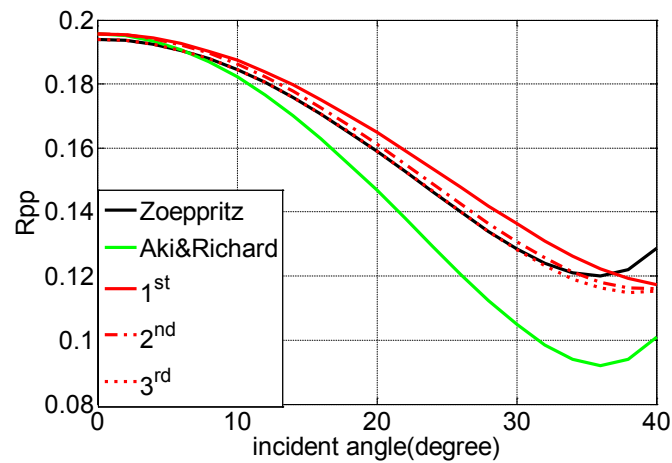


Figure 1. Comparison of approximation of R_{pp} with 1st,2nd and 3rd order in elastic parameters with elastic parameters. The exact solution for R_{pp} is calculated from Zoeppritz equation in black line. Aki&Richard approximation is indicated in green line. Approximation in series of contrast form is indicated in red line. The solid line, point dash line and point line denote the 1st, 2nd and 3rd order truncation respectively.

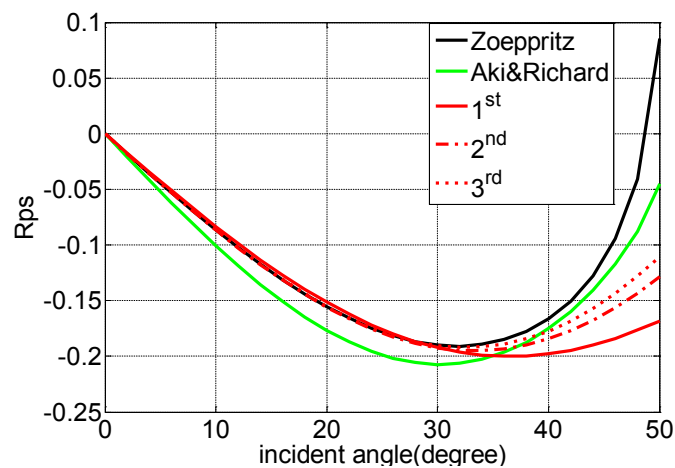


Figure 2. Comparison of approximation of R_{ps} with 1st,2nd and 3rd order in elastic parameters with elastic parameters. The exact solution for R_{ps} is calculated from Zoeppritz equation in black line. Aki&Richard approximation is indicated in green line. Approximation in series of contrast form is indicated in red line. The solid line, point dash line and point line denote the 1st, 2nd and 3rd order truncation respectively.

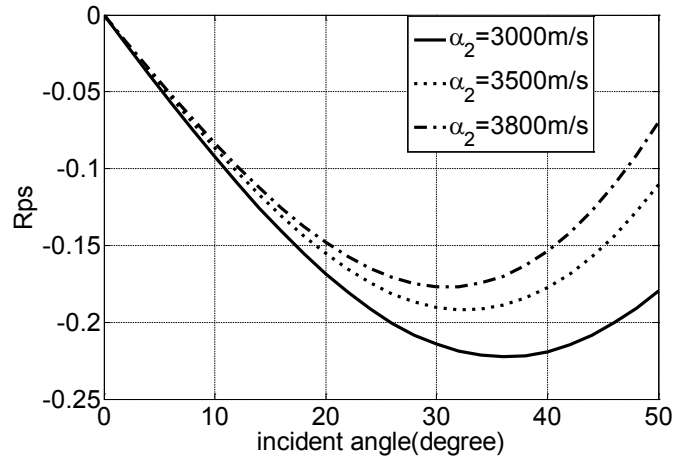


Figure 3. Effect of P wave velocity contrast on reflection coefficient of PS wave with the elastic parameters $\alpha_1 = 2700m/s$, $\beta_1 = 1300m/s$, $\rho_1 = 2.1g/cm^3$ for upper layer and $\beta_2 = 1900m/s$, $\rho_2 = 2.4g/cm^3$ for lower layer. The P wave velocity for lower layer are 3000m/s, 3500m/s and 3800m/s respectively.

AVO SERIES REVERSION

Series reversion is a way of inverting nonlinear relationships. For any function we can expand it in series, for example

$$y = \frac{x}{1-x} \approx x + x^2 + x^3 + \dots \quad (29)$$

The solution of original function for x is

$$x = \frac{y}{1+y} \quad (30)$$

The trick in solving for x with series form is to then expand each instance of x in a new series:

$$x = x_1 + x_2 + x_3 + \dots \quad (31)$$

Where x_n is defined to be that part of x which is n th order in y . Put this expansion into equation 29 and then equate like orders, consequently solve for each x_n making use of all the results for x_i ($i < n$)

$$x_1 = y$$

$$x_2 = -y^2$$

$$x_3 = y^3$$

Finally, resemble the series for x

$$x = x_1 + x_2 + x_3 + \dots = y(1 - y + y^2 - \dots) = \frac{y}{1+y} \quad (32)$$

as desired analytic solution equation 30.

By inspection of equation 15 and 16 combining equation 23 through 28, the expression of reflection coefficient of PP (R_{pp}) and PS (R_{ps}) is function of power

series of elastic parameter contrasts r_α , r_β and r_ρ . According to series reversion theory, we expand each instance of r_α , r_β and r_ρ in a new series:

$$r_\alpha = r_{\alpha 1} + r_{\alpha 2} + r_{\alpha 3} + \dots \quad (33)$$

$$r_\beta = r_{\beta 1} + r_{\beta 2} + r_{\beta 3} + \dots \quad (34)$$

$$r_\rho = r_{\rho 1} + r_{\rho 2} + r_{\rho 3} + \dots \quad (35)$$

Put those expansions into equation 23 through 28 and further into equation 15 and 16. Consequently equating like orders, we solve for each $r_{\alpha i}$, $r_{\beta i}$, $r_{\rho i}$, making use of all the results for $r_{\alpha i}$, $r_{\beta i}$, $r_{\rho i}$ ($i < n$).

for first order:

$$R_{W1} = \Gamma_{\alpha 1}^W r_{\alpha 1} + \Gamma_{\beta 1}^W r_{\beta 1} + \Gamma_{\rho 1}^W r_{\rho 1} \quad (36)$$

for second order

$$-\Delta R_2 = \Gamma_{\alpha 1}^W r_{\alpha 2} + \Gamma_{\beta 1}^W r_{\beta 2} + \Gamma_{\rho 1}^W r_{\rho 2} \quad (37)$$

$$\Delta R_2 = \Gamma_{\alpha 2}^W r_{\alpha 1}^2 + \Gamma_{\beta 2}^W r_{\beta 1}^2 + \Gamma_{\rho 2}^W r_{\rho 1}^2 + \Gamma_{\alpha 1 \beta 1}^W r_{\alpha 1} r_{\beta 1} + \Gamma_{\alpha 1 \rho 1}^W r_{\alpha 1} r_{\rho 1} + \Gamma_{\beta 1 \rho 1}^W r_{\beta 1} r_{\rho 1} \quad (38)$$

for third order

$$-\Delta R_3 = \Gamma_{\alpha 1}^W r_{\alpha 3} + \Gamma_{\beta 1}^W r_{\beta 3} + \Gamma_{\rho 1}^W r_{\rho 3} \quad (39)$$

$$\begin{aligned} \Delta R_3 = & \Gamma_{\alpha 3}^W r_{\alpha 1}^3 + \Gamma_{\beta 3}^W r_{\beta 1}^3 + \Gamma_{\rho 3}^W r_{\rho 1}^3 + \Gamma_{\alpha 2 \beta 1}^W r_{\alpha 1}^2 r_{\beta 1} + \Gamma_{\alpha 2 \rho 1}^W r_{\alpha 1}^2 r_{\rho 1} \\ & + \Gamma_{\beta 2 \alpha 1}^W r_{\beta 1}^2 r_{\alpha 1} + \Gamma_{\beta 2 \rho 1}^W r_{\beta 1}^2 r_{\rho 1} + \Gamma_{\rho 2 \alpha 1}^W r_{\rho 1}^2 r_{\alpha 1} + \Gamma_{\rho 2 \beta 1}^W r_{\rho 1}^2 r_{\beta 1} \\ & + \Gamma_{\alpha 2}^W 2r_{\alpha 1} r_{\alpha 2} + \Gamma_{\beta 2}^W 2r_{\beta 1} r_{\beta 2} + \Gamma_{\rho 2}^W 2r_{\rho 1} r_{\rho 2} + \Gamma_{\alpha 1 \beta 1}^W (r_{\alpha 1} r_{\beta 2} + r_{\alpha 2} r_{\beta 1}) \\ & + \Gamma_{\alpha 1 \rho 1}^W (r_{\alpha 1} r_{\rho 2} + r_{\alpha 2} r_{\rho 1}) + \Gamma_{\beta 1 \rho 1}^W (r_{\beta 1} r_{\rho 2} + r_{\beta 2} r_{\rho 1}) + \Gamma_{\alpha 1 \beta 1 \rho 1}^W r_{\alpha 1} r_{\beta 1} r_{\rho 1} \end{aligned} \quad (40)$$

Where superscript W is p for PP wave and s for PS wave respectively. In general, for multi-angle prestack seismic data, the AVO series reversion is carried out with four steps:

Step 1: putting multi-angle real seismic data $R_{pp}(\theta_i)$ or $R_{ps}(\theta_i)$ ($i=1,2,\dots,N$) into the left hand of equation 36, i.e. $R_{W1} = R_{pp}$ or R_{ps} and solving the solution of $r_{\alpha 1}$, $r_{\beta 1}$ and $r_{\rho 1}$.

$$\begin{aligned} R_{W1}(\theta_1) &= \Gamma_{\alpha 1}^W(\theta_1) r_{\alpha 1} + \Gamma_{\beta 1}^W(\theta_1) r_{\beta 1} + \Gamma_{\rho 1}^W(\theta_1) r_{\rho 1} \\ R_{W1}(\theta_2) &= \Gamma_{\alpha 1}^W(\theta_2) r_{\alpha 1} + \Gamma_{\beta 1}^W(\theta_2) r_{\beta 1} + \Gamma_{\rho 1}^W(\theta_2) r_{\rho 1} \\ &\vdots \\ R_{W1}(\theta_N) &= \Gamma_{\alpha 1}^W(\theta_N) r_{\alpha 1} + \Gamma_{\beta 1}^W(\theta_N) r_{\beta 1} + \Gamma_{\rho 1}^W(\theta_N) r_{\rho 1} \end{aligned} \quad (41)$$

Under condition of least square theory, the solution of $r_{\alpha 1}$, $r_{\beta 1}$ and $r_{\rho 1}$, are expressed as

$$r_1 = \left[(\Gamma_1^W)^T \Gamma_1^W \right]^{-1} (\Gamma_1^W)^T \bar{R}_{W1} \quad (42)$$

where $r_1 = [r_{\alpha 1}, r_{\beta 1}, r_{\rho 1}]^T$, $\bar{R}_{W1} = [R_{W1}(\theta_1), R_{W1}(\theta_2), \dots, R_{W1}(\theta_N)]^T$ and

$$\Gamma_1^W = \begin{bmatrix} \Gamma_{\alpha 1}^W(\theta_1) & \Gamma_{\beta 1}^W(\theta_1) & \Gamma_{\rho 1}^W(\theta_1) \\ \Gamma_{\alpha 1}^W(\theta_2) & \Gamma_{\beta 1}^W(\theta_2) & \Gamma_{\rho 1}^W(\theta_2) \\ \vdots & \vdots & \vdots \\ \Gamma_{\alpha 1}^W(\theta_N) & \Gamma_{\beta 1}^W(\theta_N) & \Gamma_{\rho 1}^W(\theta_N) \end{bmatrix}$$

Step 2: substituting solutions of $r_{\alpha 1}$, $r_{\beta 1}$ and $r_{\rho 1}$ into nonlinear corrections in equation 38 to compute ΔR_2 and then putting it into the left hand of equation 37, solving the solution of $r_{\alpha 2}$, $r_{\beta 2}$ and $r_{\rho 2}$.

$$r_2 = \left[(\Gamma_1^W)^T \Gamma_1^W \right]^{-1} (\Gamma_1^W)^T \Delta \bar{R}_2 \quad (43)$$

where $r_2 = [r_{\alpha 2}, r_{\beta 2}, r_{\rho 2}]^T$, $\Delta \bar{R}_2 = [-\Delta R_2(\theta_1), -\Delta R_2(\theta_2), \dots, -\Delta R_2(\theta_N)]^T$.

Step 3: substituting all the results for $r_{\alpha i}$, $r_{\beta i}$, $r_{\rho i}$ ($i < 3$) into nonlinear corrections in equation 40 to compute ΔR_3 and then putting it into the left hand of equation 39, solving the solution of $r_{\alpha 3}$, $r_{\beta 3}$ and $r_{\rho 3}$.

$$r_3 = \left[(\Gamma_1^W)^T \Gamma_1^W \right]^{-1} (\Gamma_1^W)^T \Delta \bar{R}_3 \quad (44)$$

where $r_3 = [r_{\alpha 3}, r_{\beta 3}, r_{\rho 3}]^T$, $\Delta \bar{R}_3 = [-\Delta R_3(\theta_1), -\Delta R_3(\theta_2), \dots, -\Delta R_3(\theta_N)]^T$.

Step 4: resembling all the results for $r_{\alpha i}$, $r_{\beta i}$, $r_{\rho i}$ ($i < 4$) into equation 33 through 35 and obtaining the solutions of r_{α} , r_{β} , r_{ρ} .

Nonlinear AVO inversion

Obviously, the AVO series reversion involves high order terms of reflection coefficient of R_{pp} and R_{ps} , but during the process of substituting equation 33 through 35 into equation 23 through 28 and equating like order, we also omit some combination of $r_{\alpha i}$, $r_{\beta i}$, $r_{\rho i}$ ($i < 1, 2, 3$), with total order greater than 2 for second order and 3 for third order. In essential, the reflection coefficient of R_{pp} and R_{ps} is expressed as the nonlinear function of elastic contrasts r_{α} , r_{β} , r_{ρ} . According to least square nonlinear inversion theory, the objective function F is sum of residuals between synthetic data R^M and real seismic data R^S for all incident angle.

$$F = \sum_{i=1}^N [R_i^M - R_i^S]^2 \quad (45)$$

where R^M is either second or third order truncated approximation for equation 15 for PP wave and equation 16 for PS wave.

The Gauss-Newton algorithm is a classic way to solve non-linear least square problem. The kth iterative step can be expressed mathematically as

$$x_{k+1} = x_k - H_k^{-1} G_k \quad (46)$$

where the x_k is the result of k-th iterative step, H_k is the Hessian matrix of the objective function F in k-th iterative step, G_k is the gradient of the objective function F in k-th iterative step, x_{k+1} is the new update parameter for k+1 iterative step.

$$x_k = [r_\alpha, r_\beta, r_\rho]_k^T \quad (47)$$

$$G_k = \left[\frac{\partial F}{\partial r_\alpha}, \frac{\partial F}{\partial r_\beta}, \frac{\partial F}{\partial r_\rho} \right]_k^T \quad (48)$$

$$H_k = \begin{bmatrix} \frac{\partial^2 F}{\partial r_\alpha^2} & \frac{\partial^2 F}{\partial r_\alpha \partial r_\beta} & \frac{\partial^2 F}{\partial r_\alpha \partial r_\rho} \\ \frac{\partial^2 F}{\partial r_\beta \partial r_\alpha} & \frac{\partial^2 F}{\partial r_\beta^2} & \frac{\partial^2 F}{\partial r_\beta \partial r_\rho} \\ \frac{\partial^2 F}{\partial r_\rho \partial r_\alpha} & \frac{\partial^2 F}{\partial r_\rho \partial r_\beta} & \frac{\partial^2 F}{\partial r_\rho^2} \end{bmatrix} \quad (49)$$

It is well known that the initial model is very important for Gauss-Newton iteration algorithm. Better initial model closed to the true value converge true value rapidly, otherwise, worse initial model may be not converge or converge to local optimization solution. How to choose to the optimized initial model is key issue. To solve this problem, we chose the solution of first or second order AVO series reversion as the initial model which helpful to converge global solution rapidly.

Experiment analysis

In this section, I illustrate the result of AVO series reversion and Gauss-Newton iterative nonlinear AVO inversion. The test model consists of five isotropic layers which parameters listed in table 1. Figure 5 shows that second layer is a lower velocity layer and fourth layer is a high velocity layer. Figure 6 illustrates synthetic of elastic contrasts r_α, r_β and r_ρ convolved wavelet with domain frequency 30Hz. The input data used to evaluate the method of AVO series reversion and nonlinear iterative inversion is angle gather for 0 to 30 at interval 5 degree computed from Zoeppritz equation convolved wavelet with domain frequency 30Hz. For convenient, here we only show the result of interface1 between layer 1 and layer 2, interface 3 between layer 3 and layer 4. For interface 1, result of r_α and r_β are smaller, otherwise, result of r_ρ is larger, than true value at first order approximation (Figure 7). In figure 8 and 9, the inversion result and relative error analysis for interface 1 are plotted versus different method. x axis denotes the first, second and third order nonlinear correction result of AVO series reversion, nonlinear iterative inversion result for third order approximation and the model value. It is clear that the accuracy of inversion result at high order approximation grows. The relative error is larger than 20% for first order approximation series reversion, otherwise near 2% for third order approximation series reversion. The nonlinear inversion using third order approximation further reduces relative error. All of the value list in table 2.

Figure 10 illustrates comparison of AVO series reversion and nonlinear iterative inversion for interface 3 between layer 3 and layer 4. It obviously agrees that the accuracy of inversion result at high order approximation grows, but different from inversion result for interface 1 which moves to model value gradually, inversion result for interface 3 moves to model value in fluctuation (figure 10 and 11). For r_α and r_β , the inversion result of first order approximation is larger than model value, but the one of second order approximation is smaller (figure 10 and 11), with decreased absolute relative error (figure 12). It is extremely attractive that for r_ρ the inversion result of first order approximation is negative which is opposite to model value and leads that relative error reaches -175.34%. But the accuracy increases at high order approximation. Similar to conclusion for interface 1, the nonlinear iterative inversion method further improve accuracy and reduce relative error. All of the value list in table 3.

Table 1 Model parameters

Layer	P wave(m/s)	S wave(m/s)	Density(kg/m ³)	Bottom depth(ms)
1	3000	1500	2300	400
2	2700	1400	2100	600
3	3000	1500	2300	800
4	3500	1700	2400	1000
5	3000	1500	2300	1200

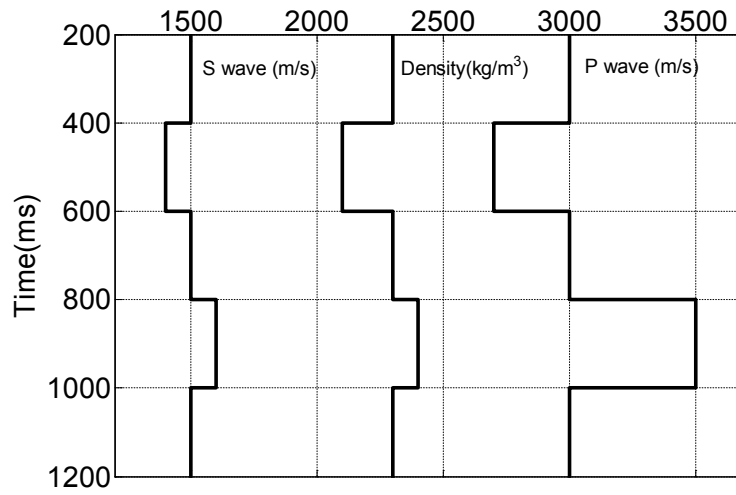


Figure 5. Logging of the test model. Second layer is a lower velocity layer and fourth layer is a high velocity layer.

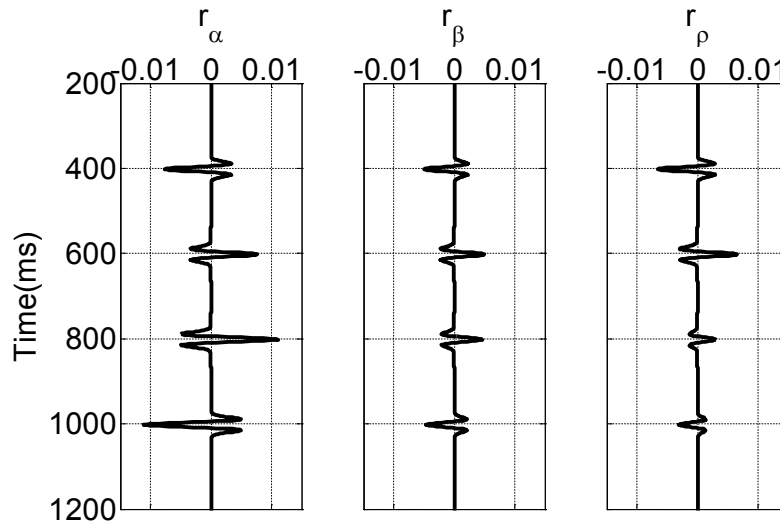


Figure 6. Synthetic of elastic contrasts r_α , r_β and r_p convolved wavelet with 30Hz domain frequency.

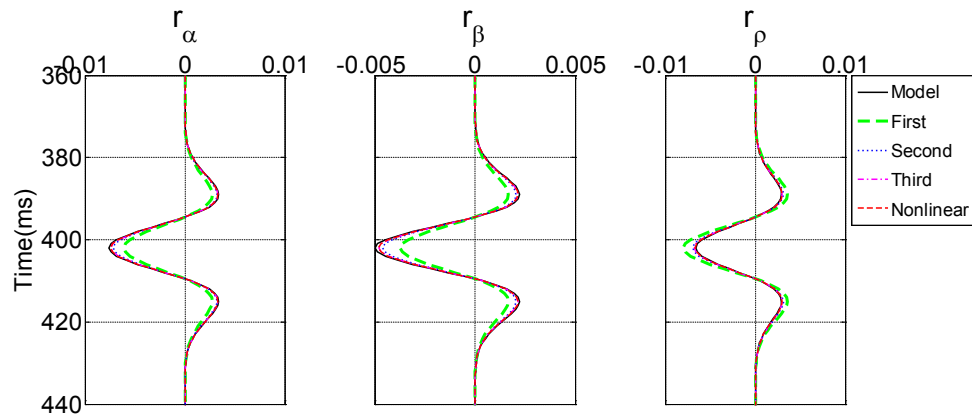


Figure 7. Comparison of AVO series reversion and nonlinear iterative inversion for interface 1 between layer 1 and layer 2.

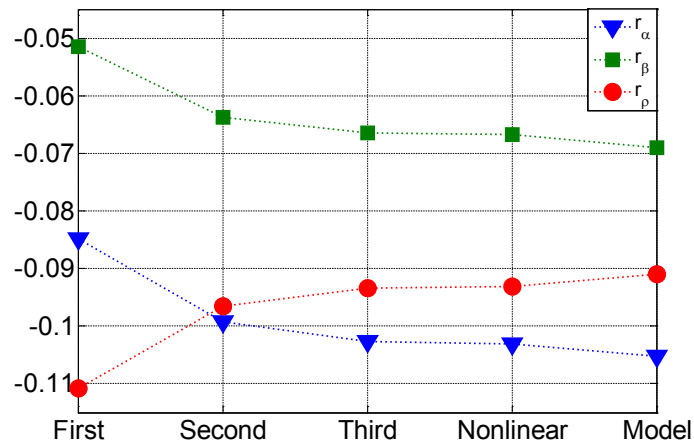


Figure 8. Display the inversion result of AVO series reversion and nonlinear iterative inversion for interface 1 between layer 1 and layer 2.

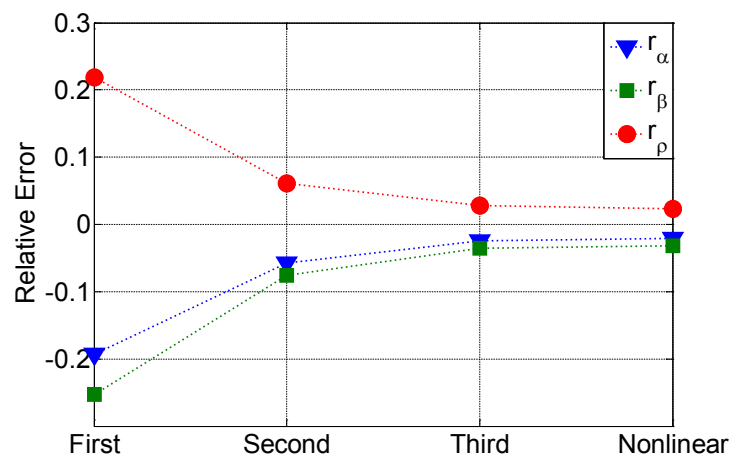


Figure 9. Display the relative error of AVO series reversion and nonlinear iterative inversion for interface 1 between layer 1 and layer 2

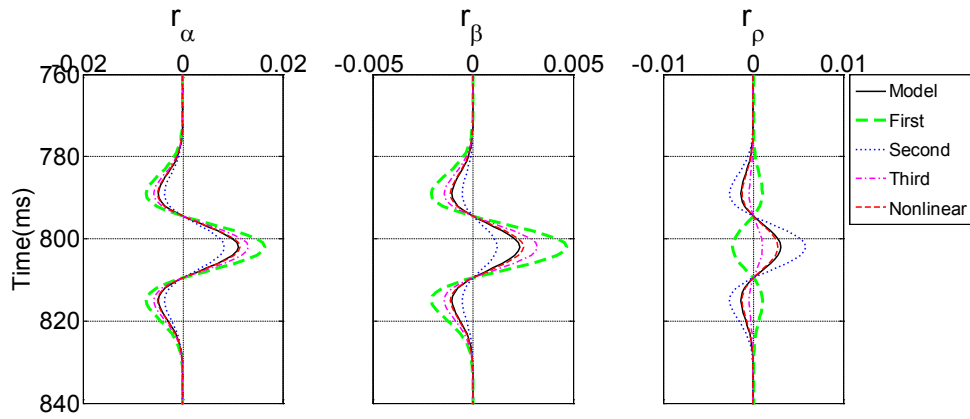


Figure 10. Comparison of AVO series reversion and nonlinear iterative inversion for interface 3 between layer 3 and layer 4.

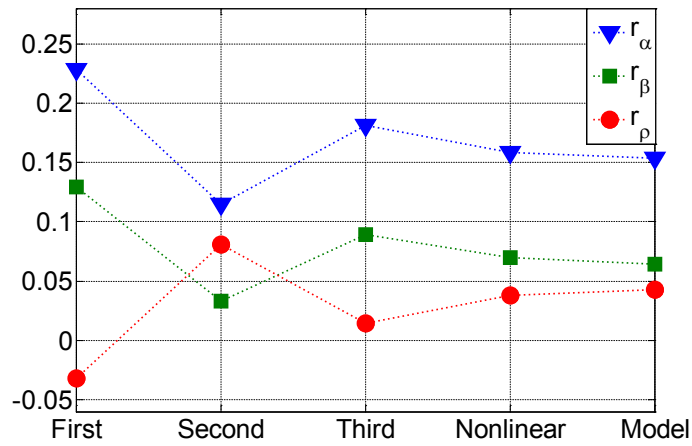


Figure 11. Display the inversion result of AVO series reversion and nonlinear iterative inversion for interface 3 between layer 3 and layer 4.

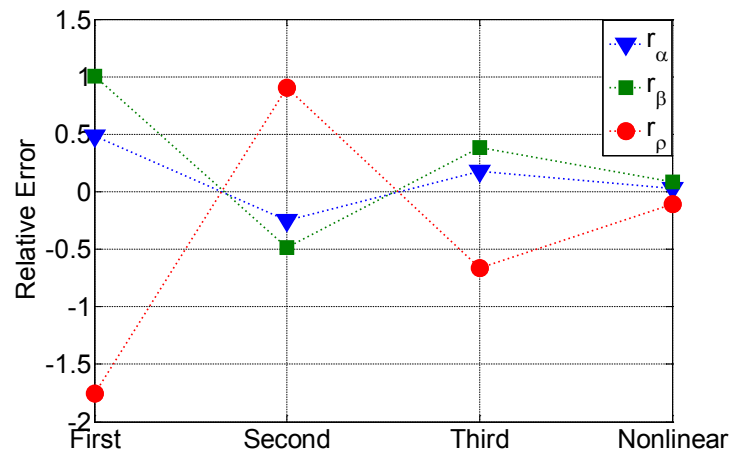


Figure 12. Display the relative error of AVO series reversion and nonlinear iterative inversion for interface 3 between layer 3 and layer 4

Table 2 Inversion result of interface 1

	Model	Inversion result				Relative error (%)			
		First	Second	Third	Nonlinear	First	Second	Third	Nonlinear
r_α	-0.1052	-0.0848	-0.0992	-0.1026	-0.1031	-19.35	-5.74	-2.44	-2.03
r_β	-0.0689	-0.0515	-0.0637	-0.0664	-0.0667	-25.31	-7.63	-3.58	-3.16
r_ρ	-0.0909	-0.1108	-0.0964	-0.0934	-0.0931	21.88	6.13	2.81	2.35

Table 3 Inversion result of interface 3

	Model	Inversion result				Relative error (%)			
		First	Second	Third	Nonlinear	First	Second	Third	Nonlinear
r_α	0.1538	0.2281	0.1150	0.1814	0.1584	48.31	-25.22	17.92	2.96
r_β	0.0645	0.1294	0.0330	0.0892	0.0699	100.64	-48.71	38.39	8.41
r_ρ	0.0425	-0.0320	0.0810	0.0143	0.0379	-175.34	90.47	-66.35	-10.72

CONCLUSION

In this paper, we have carried out a high accuracy AVO inversion using high order series expansion and approximation formulas. A new AVO series expansions derived from Zoeppritz equation describe the reflection coefficient of PP (R_{pp}) and PS wave (R_{ps}) as function of elastic parameter contrasts $r_\alpha, r_\beta, r_\rho$ and incident angle θ . The coefficient of r_α, r_β and r_ρ derived in this paper is same as the one in Aki&Richard approximation or other derived approximation except that the average angle of incident and transmission angle is replaced by incident angle. The replacement is more directly help us to map offset to angle in AVO inversion process workflow. In other hand, deviation of average angle from incident angle increases with contrasts in elastic parameter across interface. So the new series expansions formulas have more high accuracy than Aki&Richard approximation or other derived approximation at small range of incident angle, especially for strong contrasts in elastic parameters.

For converted wave (PS), contrast in P wave velocity plays a small but nonnegligible role in determining the reflection coefficient R_{ps} at small and moderate angle in second and third order terms. It's influence is enacted through coupling with the density and S wave velocity.

The series expansion allows us to add terms to generate numerically more accurate approximations of seismic amplitude. This feature in turn allows us to reconstruct contrasts in elastic parameters from seismic amplitude at range of incident angle. The first order truncated approximation is a linear equation similar to traditional linear AVO equations except to replace average angle between incident and transmission angle with incident angle. AVO series reversion method is to expand the contrasts $r_\alpha, r_\beta, r_\rho$ themselves in series. These series are substituted into series expansion of reflection coefficient and like orders are equated following the argumentation applied in inverse scatter theory. The experiments indicate that recovery of first order $r_{\alpha 1}, r_{\beta 1}, r_{\rho 1}$ from linear approximation may be larger or smaller than the model value. Those first order $r_{\alpha 1}, r_{\beta 1}, r_{\rho 1}$ are substituted into equation 38 to generate nonlinear correction term ΔR_2 , and then reconstructions of second order $r_{\alpha 2}, r_{\beta 2}, r_{\rho 2}$ are carried out using equation 37. It is evident that the accuracy of inversion result at second order approximation grows. Consequently, the first and second order of contrasts are substituted into equation 40 to generate nonlinear correction term ΔR_3 ,

and then reconstructions of second order $r_{\alpha 3}, r_{\beta 3}, r_{\rho 3}$, are performed using equation 39. The nonlinear inversion using third order approximation further increase accuracy. Theoretically, this series reversion procedure may continue to any desired order. But nonlinear correction for high order is more complex and difficult to give analytic expression. Alternatively, high order series expansion of reflection coefficient are also nonlinear function of contrasts in elastic parameters, Gauss-Newton iteration method are well known effective approach to resolve the nonlinear problem. To solve for the local convergence problem of Gauss-Newton iteration method, we introduce the first or second AVO series reversion result as the initial value. All of the experiments illustrate that reconstruction of contrasts from Gauss-Newton iteration nonlinear AVO inversion is more accuracy then series reversion. But we must keep in mind that third order series reversion also gives a more satisfied result and series reversion is linear algorithm which run faster than Gauss-Newton iteration method.

ACKNOWLEDGEMENTS

This work was funded by CREWES and SINOPEC. CREWES sponsors and all research personnel are gratefully acknowledged.

REFERENCE

- Chen, Tiansheng, Xiucheng Wei, and others. 2012. "Zeoppritz-Based Joint AVO Inversion of PP and PS Waves in Ray Parameter Domain." SEG Annual Meeting. Society of Exploration Geophysicists.
- Connolly, Patrick. 1999. "Elastic Impedance." *The Leading Edge* 18 (4): 438–52.
- Downton, Jonathan E. 2005. *Seismic Parameter Estimation from AVO Inversion*, PHD, University of Calgary.
- Goodway, Bill. 1999. "Improved AVO Fluid Detection and Lithology Discrimination Using Lamé Petrophysical Parameters; $\lambda\rho'$, $\mu\rho'$, & λ/μ Fluid Stack', from P and S Inversions." In SEG Technical Program Expanded Abstracts.
- Innanen, Kristopher A. 2011. "Inversion of the Seismic AVF/AVA Signatures of Highly Attenuative Targets." *Geophysics* 76 (1): R1–14.
- Jin, Side, G Cambois, and C Vuillermoz. 2000. "Shear-Wave Velocity and Density Estimation from PS-Wave AVO Analysis: Application to an OBS Dataset from the North Sea." *Geophysics* 65 (5): 1446–54.
- Larsen, Jeffrey A. 1999. "AVO Inversion by Simultaneous PP and PS Inversion." M. Sc. Thesis, University of Calgary.
- Lines, Laurence R. 1998. "Density Contrast Is Difficult to Determine from AVO." *Canadian Journal of Exploration Geophysics*.
- Russell, Brian H, Ken Hedlin, Fred J Hilterman, and Lawrence R Lines. 2003. "Fluid-Property Discrimination with AVO: A Biot-Gassmann Perspective." *Geophysics* 68 (1): 29–39.
- Smith, GC, and PM Gidlow. 1987. "Weighted Stacking for Rock Property Estimation and Detection of Gas." *Geophysical Prospecting* 35 (9): 993–1014.
- Smith, George C, and others. 1996. "3-Parameter Geostack." SEG Annual Meeting. Society of Exploration Geophysicists.
- Wang, Youjiang. 2003. *Seismic Amplitude Inversion in Reflection Tomography*. Elsevier.
- Zhang, F, and Y Wang. 2010. "Ray Impedance Inversion on the Tight-Sand Gas Reservoir." In 72nd EAGE Conference and Exhibition Incorporating SPE EUROPEC 2010.
- Zhang, Haiyan, and Arthur B. Weglein. 2009. "Direct Nonlinear Inversion of Multiparameter 1D Elastic Media Using the Inverse Scattering Series." *Geophysics* 74 (6): WCD15–27.
- Zoeppritz, K. 1919. "Erdbebenwellen VIII B. Über Reflection and Durchgang Seismischer Wellen Durch Unstetigkeitsflächen." *Göttinger Nachrichten*, 66–84.

APPENDIX A

The coefficients in the expansion for PP wave in equation 33 through 35 are:

$$\Gamma_{\alpha 1} = \frac{1}{2} \sec^2 \theta \quad \Gamma_{\beta 1} = -4B \sin^2 \theta \quad \Gamma_{\rho 1} = \frac{1}{2} - 2B^2 \sin^2 \theta$$

$$\begin{aligned} \Gamma_{\alpha 2} &= \frac{1}{2} \sin^2 \theta & \Gamma_{\beta 2} &= 4B^2 (B-1) \sin^2 \theta & \Gamma_{\rho 2} &= \frac{1}{4} B(4B^2 - 1) \sin^2 \theta \\ \Gamma_{\alpha 1 \beta 1} &= 0 & \Gamma_{\alpha 1 \rho 1} &= 0 & \Gamma_{\beta 1 \rho 1} &= 2B^2 (2B-1) \sin^2 \theta \\ \Gamma_{\alpha 3} &= \frac{1}{4} \sin^2 \theta & \Gamma_{\beta 3} &= 3B^2 (2B-1) \sin^2 \theta & \Gamma_{\rho 3} &= -\frac{1}{8} B(4B^2 - 4B + 1) \sin^2 \theta \\ \Gamma_{\alpha 2 \beta 1} &= B^2 \sin^2 \theta & \Gamma_{\alpha 2 \rho 1} &= -\frac{1}{8} + \left(\frac{1}{2} B^2 - \frac{1}{4} \right) \sin^2 \theta \\ \Gamma_{\beta 2 \alpha 1} &= -4B^2 \sin^2 \theta & \Gamma_{\beta 2 \rho 1} &= B^2 (4B-1) \sin^2 \theta \\ \Gamma_{\rho 2 \alpha 1} &= -\frac{1}{8} + \left(-B^3 + B^2 - \frac{1}{4} B - \frac{1}{8} \right) \sin^2 \theta & \Gamma_{\rho 2 \beta 1} &= -\frac{1}{8} B(4B^2 - 12B + 1) \sin^2 \theta \\ \Gamma_{\alpha 1 \beta 1 \rho 1} &= -2B^2 (2B-1) \sin^2 \theta \end{aligned}$$

The coefficients in the expansion for PS wave in equation 36 through 38 are:

$$\begin{aligned} \Gamma_{\alpha 1} &= 0 \\ \Gamma_{\beta 1} &= -2BX + B(2B+1)X^3 \\ \Gamma_{\rho 1} &= (-B-1/2)X + (3/4B^2 + B/2)X^3 \\ \Gamma_{\alpha 2} &= 0 \\ \Gamma_{\beta 2} &= -BX - 1/2B(14B^2 - 6B-1)X^3 \\ \Gamma_{\rho 2} &= (B/2 - 1/4)X + \left(-2B^3 + \frac{11B^2}{8} - B/4 \right) X^3 \\ \Gamma_{\alpha 1 \beta 1} &= BX + 1/2B(2B+1)X^3 \\ \Gamma_{\alpha 1 \rho 1} &= (B/2 - 1/4)X + (3/8B^2 + B/4 - 1/4)X^3 \\ \Gamma_{\beta 1 \rho 1} &= (B/2 - 1/4)X + \left(-15/2B^3 + \frac{33B^2}{8} - B/4 \right) X^3 \\ \Gamma_{\alpha 3} &= 0 \\ \Gamma_{\beta 3} &= -1/2BX + 1/4B(32B^3 - 56B^2 + 10B+1)X^3 \\ \Gamma_{\rho 3} &= 1/8B(8B^3 - 4B^2 - 2B+1)X^3 \\ \Gamma_{\alpha 2 \beta 1} &= BX^3 \\ \Gamma_{\alpha 2 \rho 1} &= (B/2 - 1/4)X^3 \\ \Gamma_{\beta 2 \alpha 1} &= 1/2BX - 1/4B(2B^2 - 6B-1)X^3 \\ \Gamma_{\beta 2 \rho 1} &= 1/2BX + 1/4B(48B^3 - 68B^2 + 17B-1)X^3 \\ \Gamma_{\rho 2 \alpha 1} &= 0 \\ \Gamma_{\rho 2 \beta 1} &= 1/2BX + 1/4B(24B^3 - 24B^2 + 4B-1)X^3 \\ \Gamma_{\alpha 1 \beta 1 \rho 1} &= (B/4 - 1/8)X + \left(-1/4B^3 + \frac{9B^2}{16} + B/8 - 1/8 \right) X^3 \end{aligned}$$